The RIP-like kinase, RIP3, induces apoptosis and NF-κB nuclear translocation and localizes to mitochondria

Gary M. Kasof, Judith C. Prosser, Derong Liu, Matthew V. Lorenzi, Bruce C. Gomes*

AstraZeneca Pharmaceuticals, Enabling Science and Technology Department, 1800 Concord Pike, Wilmington, DE 19803, USA

Received 18 February 2000; received in revised form 6 March 2000

Edited by Vladimir Skulachev

Abstract A RIP-like protein, RIP3, has recently been reported that contains an N-terminal kinase domain and a novel C-terminal domain that promotes apoptosis. These experiments further characterize RIP3-mediated apoptosis and NF-κB activation. Northern blots indicate that *rip*3 mRNA displays a restricted pattern of expression including regions of the adult central nervous system. The *rip*3 gene was localized by fluorescent in situ hybridization to human chromosome 14q11.2, a region frequently altered in several types of neoplasia. RIP3-mediated apoptosis was inhibited by Bcl-2, Bcl-x_L, dominant-negative FADD, as well as the general caspase inhibitor Z-VAD. Further dissection of caspase involvement in RIP3-induced apoptosis indicated inhibition by the more specific inhibitors Z-DEVD (caspase-3, -6, -7, -8, and -10) and Z-VDVAD (caspase-2). However, caspase-1, -6, -8 and -9 inhibitors had little or no effect on RIP3-mediated apoptosis. Mutational analysis of RIP3 revealed that the C-terminus of RIP3 contributed to its apoptotic activity. This region is similar, but distinct, to the death domain found in many pro-apoptotic receptors and adapter proteins, including FAS, FADD, TNFR1, and RIP. Furthermore, point mutations of RIP3 at amino acids conserved among death domains, abrogated its apoptotic activity. RIP3 was localized by immunofluorescence to the mitochondrion and may play a key role in the mitochondrial disruptions often associated with apoptosis.

Key words: Cell death; Death domain; Chromosome 14q11.2; Tumor necrosis factor

1. Introduction

Tumor necrosis factor-receptor 1 (TNF-R1) and Fas/Apo-1/CD95 are prototypic members of a family of cell surface receptors that modulate physiological processes such as inflammation, immunoregulation, and anti-viral responses through the regulation of apoptosis, a genetically controlled process of cell suicide [1]. Apoptosis triggered by these receptors is dependent on a conserved cytoplasmic region of about 80 amino acids termed the 'death domain' that recruits of other death domain adapter proteins, such as TRADD, FADD, and RIP to the receptor complex. This subsequently leads to the activation of cysteine proteases, or caspases, which play a critical role in apoptosis by cleaving proteins involved in the disassembly of the cell structures. In addition to triggering an apoptotic signal, TNF-α also induces the activation of the transcription factor, NF-κB, which plays a critical role in regulating inflammatory responses [1]. Transcriptional regulation by NF-κB can suppress TNF-α-induced apoptosis and may be the dominant pathway following TNF-α treatment. In fact, many cells require the presence of RNA or protein synthesis inhibitors to elicit TNF-α-mediated apoptosis, suggesting that additional cellular signals are required for apoptosis to predominate in response to TNF-α.

RIP [2–4], and related proteins, RIP2/RICK/CARDIAK [5–7], and RIP3 [8,9], are serine/threonine kinases that contribute to both TNF-α-mediated apoptosis and NF-κB activation. The process of RIP-mediated apoptosis involves binding to the adapter molecule RAIDD/CRADD [10,11]. RAIDD contains a death domain, involved in the interaction with RIP, and a caspase recruitment domain (CARD), which binds to and activates caspase-2. The CARD domain is structurally similar to the death domain and is involved in self-association with other CARD domains found in the pro-domain of some caspases [12,13]. Thus, RIP interaction with RAIDD leads to the binding and activation of caspase-2 triggering a caspase cascade similar to, but likely distinct from, that initiated by caspase-8 through FADD. Like RIP, RIP2 contains a kinase domain, but instead of a death domain, RIP2 contains a CARD domain. RIP2 does not interact with RAIDD, but instead activates caspase-8 and caspase-1 through the CARD domain. RIP3 was identified based on homology and interaction with RIP, and like the related proteins it contains an N-terminal kinase domain. RIP3 also has a unique C-terminus that contributes to apoptosis and binding to RIP. These experiments further dissect the role of RIP3 in apoptosis and NF-κB activation.

2. Materials and methods

2.1. Identification of RIP3 and generation of expression constructs

RIP3 was identified from a homology search of the proprietary Incyte Lifeseq database with death domain containing kinases, RIP and Pelle, using the BLAST algorithm. Two Incyte clones were detected (accession numbers 1626570 and 2301422). Clone number 2301422 was verified to contain the full-length mRNA and included an in-frame stop codon in the 5′-untranslated regions (UTR). The coding sequence of wild-type and mutant (K50A, W434A/W477A, and ΔC420) RIP3 constructs were sub-cloned into pTracer-SV-40 (Invitrogen, Carlsbad, CA, USA) containing the green fluorescent protein (GFP) marker. Sub-cloning was performed by polymerase chain reaction (PCR) from Incyte clone 2301422 using the Advantage HF PCR kit (Clontech, Palo Alto, CA, USA) and then ligated into the *Eco*RV/*Not*I sites in pTracer-SV-40. The plasmids encoding a C-terminal hemagglutinin (HA)-tagged RIP3 and K50A were prepared by PCR and ligated into the *Kpn*I/*Not*I sites in the vector, pMH (Boehringer Mannheim, Indianapolis, IN, USA). Human RIP was cloned by PCR from a human monocyte cDNA library (Clontech, Palo Alto, CA, USA) and also ligated into pMH via *Hin*dIII/*Eco*RI sites. The human *bax* gene was obtained from Incyte (accession number

*Corresponding author. Fax: (1)-302-886 8830.
E-mail: bruce.gomes@phwilm.zeneca.com

PII: S0014-5793(00)01473-3

3334311) and sub-cloned into the *Eco*RV/*Not*I sites in pTracer-SV-40. Human *bcl*-x_L and *bcl*-2 were also obtained from Incyte (accession numbers 1855683 and 395314 respectively) and cloned into the mammalian expression vector pZeo-SV2 (Invitrogen, Carlsbad, CA, USA) driven by the SV-40 promoter and lacking the GFP marker. Dominant-negative FADD was designed as reported previously [14] lacking the N-terminal death effector domain (amino acids 1–79) and was prepared by PCR from Incyte clone 2057308 and ligated into the *Eco*RI/*Not*I sites in pZeo-SV2. The nucleotide sequences of all of the clones were confirmed by fluorescent terminator cycle sequencing using an automated 377 DNA sequencer (Perkin-Elmer, Applied Biosystems, Foster City, CA, USA).

2.2. Northern blotting

Northern blots (Clontech, Palo Alto, CA, USA) containing human poly-A^+ RNA (2 μg per lane) prepared from various adult human tissues were hybridized to random primed radiolabeled *rip*3 or *actin* cDNAs. Hybridizations were performed with Hybrisol I (Oncor, Gaithersburg, MD, USA) incubated overnight at 42°C. The blots were washed with 2×SSC+0.05% SDS at room temperature followed by high stringency washing, 0.1×SSC+0.1% SDS at 50°C. Blots were visualized using a Phosphorimager (Molecular Dynamics, Sunnyvale, CA, USA).

2.3. Fluorescent in situ hybridization (FISH)

The sub-chromosomal location of *rip*3 was determined by PCR screening of a human genomic library in a bacterial artificial chromosome (BAC) vector (Genome Systems, St. Louis, MO, USA) using primers 5′-TGGTATAATCATAGCGGGA-3′ (positions 1744–1762) and 5′-AGCATTCCATCATGTTTAT-3′ (positions 1898–1916). Positive BAC clones were sequenced to confirm the presence of *rip*3 and subsequently labeled with digoxigenin-dUTP by nick translation and used in FISH. FISH was performed from metaphase chromosomes derived from PHA stimulated peripheral blood leukocytes (PBL) in a solution containing 50% formamide, 10% dextran sulfate and 2×SSC. Specific hybridization signals were detected by incubating the slides in fluoresceinated anti-digoxigenin antibodies followed by counterstaining with DAPI.

2.4. Laser scanning cytometric analysis of cell death

HeLa cells (ATCC, Rockville, MD, USA) were cultured in Dulbecco's modified Eagle's medium (DMEM) supplemented with 10% fetal bovine serum (FBS) and penicillin (100 U/ml)/streptomycin (0.1 mg/ml) and maintained at 37°C/5% CO_2. Transient transfections were performed using the Lipofectamine Plus system (Life Technologies, Grand Island, NY, USA) according to manufacturer's specifications. Stock solutions (100 mM) of the caspase inhibitors, Z-VAD-FMK, Z-DEVD-FMK, Z-IETD-FMK, Z-VEID-FMK, and Z-VDVAD-FMK (Enzyme Systems, Livermore, CA, USA) were prepared in DMSO and added to the cultures 3 h post-transfection (200 μM final volume). Twenty-four hours post-transfection the cells were fixed with 2% paraformaldehyde in PBS, counterstained with 10 μg/ml propidium iodide, 200 μg/ml RNase A, and 0.1% Tween-20 for 30 min at room temperature, and then mounted with Immu-mount (Shandon, Pittsburgh, PA, USA). A laser scanning cytometer (LSC; CompuCyte, Cambridge, MA, USA) was used to determine the percent of GFP-positive cells. The propidium iodide staining served as a marker required for gating the cell population. Relative fluorescence values were determined with an excitation at 488 nm using an argon laser and emission filters at 505–540 nm (GFP) and 614–639 nm (propidium iodide). Staining was confirmed by microscopically re-locating cells within the gated regions.

2.5. Immunofluorescence

HeLa cells grown on coverslips were transfected with pMH-*rip*3, pMH-*rip*, or empty pMH vector, encoding a C-terminal HA tag. Transfectants were incubated with the caspase inhibitors Z-DEVD-FMK and Z-VAD-FMK (200 μM) to inhibit apoptosis. Twenty-four hours post-transfection the cells were incubated with the mitochondrial dye, Mitotracker Red CMXRos (500 nM; Molecular Probes, Eugene, OR, USA) for 20 min at 37°C. The cells were then fixed with 2% paraformaldehyde and permeabilized with 0.2% Triton X-100 in PBS. Coverslips were incubated with a mouse monoclonal antibody against the HA tag (Boehringer Mannheim, Indianapolis, IN, USA) for 1 h at 37°C. Co-staining with NF-κB was performed using a rabbit polyclonal antibody against NF-κB (Santa Cruz Biotechnology, Inc., Santa Cruz, CA, USA). Treatment with TNF-α (1500 U/ml; Calbiochem, La Jolla, CA, USA) for 5 h served as a positive control for the nuclear translocation of NF-κB. Staining for the HA-tagged proteins and NF-κB were detected using FITC-conjugated goat anti-mouse (Life Technologies, Grand Island, NY, USA) and Cy-3-conjugated goat anti-rabbit antibodies (Jackson Immunoresearch, West Grove, PA, USA) incubated for 1 h at 37°C. The cells were visualized by epifluorescence using an Olympus AX70 microscope equipped with a Sony DKC-5000 CCD camera (Hitech Instruments, Inc., Edgemont, PA, USA).

3. Results and discussion

3.1. Identification, expression, and chromosomal localization of rip3

We identified the *rip*3 cDNA through BLAST searches of a proprietary (Incyte) database for homologues to RIP family of death-promoting kinases. The nucleotide sequence was identical to that recently reported for *rip*3 and encoded a 518 amino acid protein containing an N-terminal serine/threonine kinase domain between amino acids 1 and 279 [18,19]. The clone contained an in-frame stop codon in the 5′-untranslated region (UTR) suggesting that it encoded a full-length protein.

The tissue distribution of *rip*3 was determined by Northern blotting with mRNA prepared from 16 different adult human tissues. Using the entire cDNA coding sequence of *rip*3 as a probe, two distinct mRNAs of approximately 2.1 kb and 2.6 kb were detected (Fig. 1). The shorter of these transcripts

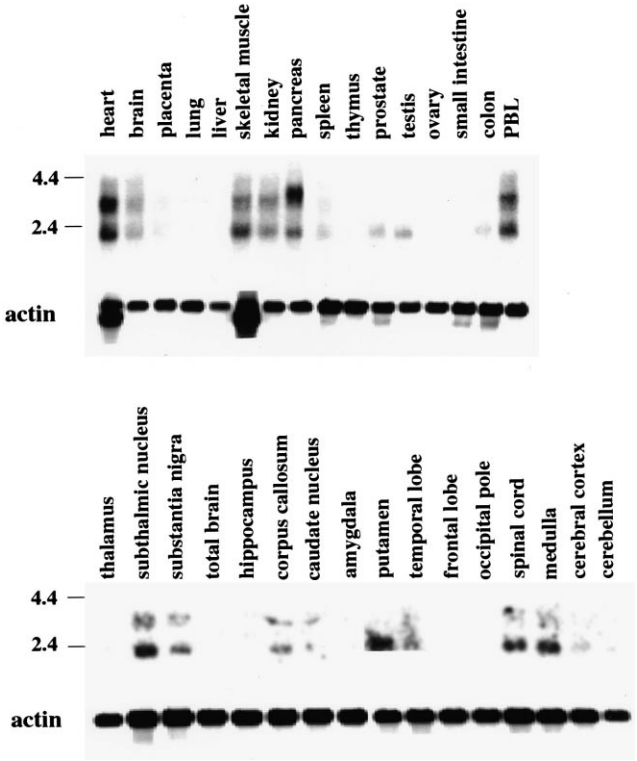

Fig. 1. Expression of *rip*3. Northern blots were performed from commercially available multiple tissue and CNS blots (Clontech). Each lane contains 2 μg of poly-A^+ RNA. Blots were probed with a cDNA sequence containing the entire coding region of *rip*3. Two transcripts were identified at 2.0 and 3.5 kb. The loading efficiency and quality of the RNA were monitored by actin hybridization. PBL, peripheral blood leukocytes.

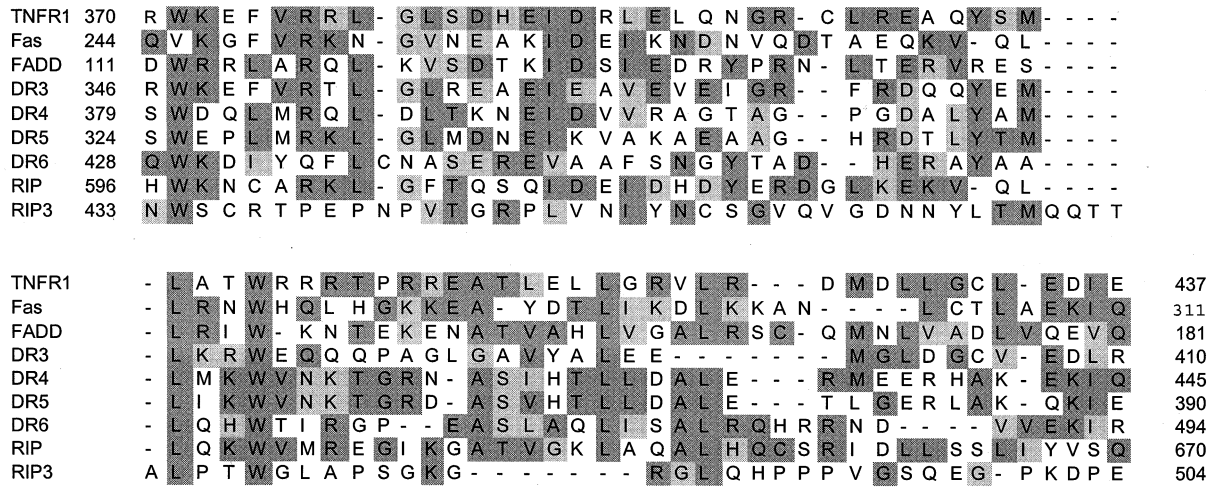

Fig. 2. Homology of the C-terminus of RIP3 with death domains. Shown here are the alignments of RIP3 with other known death domains containing proteins generated using the Clustal algorithm from the MegAlign software (DNA Star). Dark shading indicates identical residues among family members, while lighter shading represents similar amino acids.

was consistent with the identified full-length clone from the Incyte database. The nature of the larger transcript is still unknown. Expression of *rip*3 was observed in the heart, brain, placenta, skeletal muscle, kidney, pancreas, spleen, and PBL. In addition, the 2.1 kb *rip*3 transcript was detected at low levels within the prostate, testis, and colon. We were unable to detect *rip*3 in the lung, liver, thymus, ovary, and small intestine, although previous reports have shown expression in the lung and liver [9]. To investigate the expression pattern of *rip*3 in more detail, we probed several cancer cell lines as well as specific regions within the central nervous system (CNS). The *rip*3 mRNA was not detected by Northern blot in any of 23 cancer lines examined, although it could be detected by RT-PCR in some cases (data not shown). However, analysis of *rip*3 levels within the CNS did reveal some expression, particularly the smaller transcript, in several regions, including the subthalamic nucleus, substantia nigra, corpus callosum, putamen, spinal cord, and medulla suggesting a specialized role of RIP3 in these structures (Fig. 1). Thus, expression of *rip*3 was restricted in a tissue specific manner. Furthermore, the pattern of *rip*3 expression was different to that reported for *rip* and *rip*2 suggesting that tissue specificity may provide distinct roles for these related genes [2,4,5].

To further investigate a link between *rip*3 and disease, the chromosomal location of *rip*3 was determined by FISH. PCR primers containing the 3′-UTR of *rip*3 were used to screen a human genomic BAC library which was then used as a probe for FISH analysis. A single FISH signal at 14q11.2 was detected in 14 of 15 metaphase spreads from human chromosomes (data not shown). Lesions at this chromosomal locus are frequently associated with several types of cancer, particularly nasopharyngeal carcinoma [15] and several leukemias/lymphomas [16–18]. This is consistent with the lack of *rip*3 expression in any of 23 cancer cell lines that we examined. Further investigation will be required to determine the role of RIP3 in tumor progression and/or maintenance.

3.2. RIP3-mediated apoptosis in HeLa cells

Previous studies have shown that overexpression of RIP3, like RIP and RIP2, can induce cell death [18,19]. We attempted to extend these results by analyzing the apoptotic activity of some missense and deletion mutants of RIP3 as well as evaluating the effects of potential apoptotic inhibitors. Wild-type and mutant *rip*3 were cloned into the GFP containing vector pTracer-SV-40. The percent of GFP-positive cells, determined with a laser scanning cytometer, provided an indication of relative viability. Viability in RIP3 transfected cells was reduced to ~26% as compared to an empty pTracer-SV-40 vector (Table 1). The apoptotic activity of RIP3 was comparable to the pro-apoptotic Bcl-2 family member, Bax (Table 1). RIP3 transfected cells also produced an increase in TUNEL staining indicating that these cells were dying apoptosis

Table 1
Characterization of Rip3-mediated apoptosis

Treatment	% Relative viability
pTracer-SV-*bax*	26.6 ± 8.2
pTracer-SV-40-*rip*3	26.7 ± 3.0
pTracer-SV-40-*rip*3-K50A	24.9 ± 4.5
pTracer-SV-40-*rip*3-ΔC421	51.4 ± 1.4
pTracer-SV-40-*rip*3-W435A, W478A	71.8 ± 2.3
pTracer-SV-40-*rip*3+pZeo	22.8 ± 1.1
pTracer-SV-40-*rip*3+pZeo-*bcl*-2	69.5 ± 3.6
pTracer-SV-40-*rip*3+pZeo-*bcl*-x_L	68.8 ± 11.2
pTracer-SV-40-*rip*3+pZeo-FADD-DN	54.5 ± 3.2
pTracer-SV-40-*rip*3+DMSO	18.7 ± 3.0
pTracer-SV-40-*rip*3+Z-VAD-FMK	50.0 ± 0.8
pTracer-SV-40-*rip*3+Z-DEVD-FMK	35.0 ± 6.2
pTracer-SV-40-*rip*3+Z-IETD-FMK	22.8 ± 4.3
pTracer-SV-40-*rip*3+Z-VEID-FMK	20.3 ± 10.0
pTracer-SV-40-*rip*3+Z-VDVAD-FMK	39.4 ± 5.4

HeLa cells (2×10^5) were transfected with 1 μg of pTracer-SV-40 derived plasmids containing *bax*, *rip*3, mutants ΔC420, K50A, or W434/W47, or empty vector. Inhibition studies were performed by co-transfecting 1 μg of pTracer-SV-40-*rip*3 with 1 μg of *bcl*-2, *bcl*-x_L, FADD-DN or the empty pZeo vector. Also as indicated pTracer-SV-40-*rip*3 transfected cells were incubated with 200 μM of the caspase inhibitors, Z-VAD-FMK, Z-DEVD-FMK, Z-IETD-FMK, Z-VEID-FMK, Z-VDVAD-FMK, or 0.2% DMSO control. Twenty-four hours post-transfection the cells were fixed and the percent of GFP-positive cells was determined by laser scanning cytometry. At least 6000 cells were counted for each sample. The percent relative viability is the percent of GFP-positive cells compared to empty vector controls (pTracer-SV-40 with or without DMSO). $N = 3$.

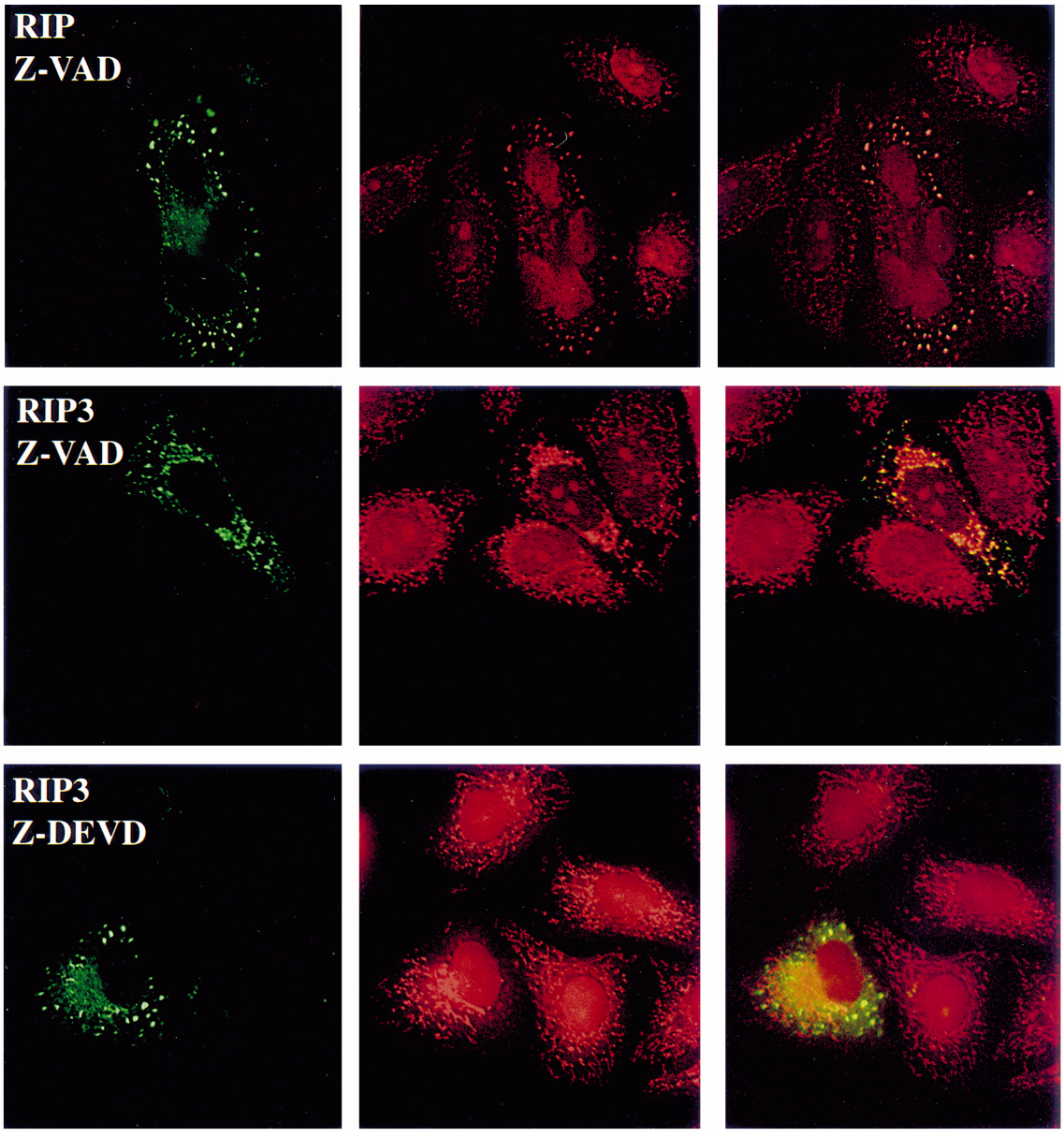

Fig. 3. Sub-cellular localization of RIP3. HeLa cells (2×10^5) were transfected with 1 μg of pMH-*rip*3 or pMH-*rip* plasmids which contain HA epitope tags. Transfected cells were incubated with 200 μM of the caspase inhibitors Z-VAD-FMK or Z-DEVD-FMK. Twenty-four hours post-transfection, the cells were incubated with Mitotracker Red CMX (500 nM) for 20 min at 37°C and then immuno-stained using a mouse monoclonal HA antibody followed by a FITC-conjugated goat anti-mouse antibody. Micrographs (60× objective) show epitope staining of RIP/RIP3 (left), Mitotracker staining (middle), and a composite of the two panels performed using Adobe Photoshop (right).

(data not shown). Disruption of RIP3-mediated kinase activity by amino acid substitution of the putative ATP-binding site, lysine to alanine at position 50 (K50A) [8,9], had no effect on RIP3-triggered apoptosis (Table 1). In contrast, both missense and deletion mutations within the C-terminus significantly attenuated its apoptotic activity. A deletion mutant lacking amino acids 422–519 (ΔC420) decreased RIP3 apoptotic activity. Indeed, the C-terminus of RIP3 previously was shown to contribute to apoptosis and interaction with death domain containing proteins [8,9]. This region of RIP3 has some homology to death domains which may explain its apoptotic activity as well as its ability to bind to other death domain containing proteins (Fig. 2). The C-terminal region of RIP3 contains several residues, which by mutagenesis of Fas and TNF-R1, were shown to be critical for death domain interactions and cytotoxicity like the tryptophan residue at position 477, the leucine residues at 474 and 488 [12]. RIP3 also contains several highly conserved residues like tryptophan 434, valine 444, threonine 445, leucine 449, and isoleucine 452. The conserved valine residue at position 444 of RIP3 is the site of a naturally occurring mutation within Fas that leads to lymphoproliferation syndrome in mice [19]. However, RIP3 does not contain several highly conserved residues which were critical for either Fas or TNF-R1 function, such as arginine 376, leucine 378, alanine 416, and leucine 421 (positions corresponding to TNF-R1). In addition, RIP3 contains several proline residues which may disrupt the α-helical structure of the death domain. Thus, it is unlikely that RIP3 forms a typical death domain structure. Nonetheless, to determine if this region could function similar to a death do-

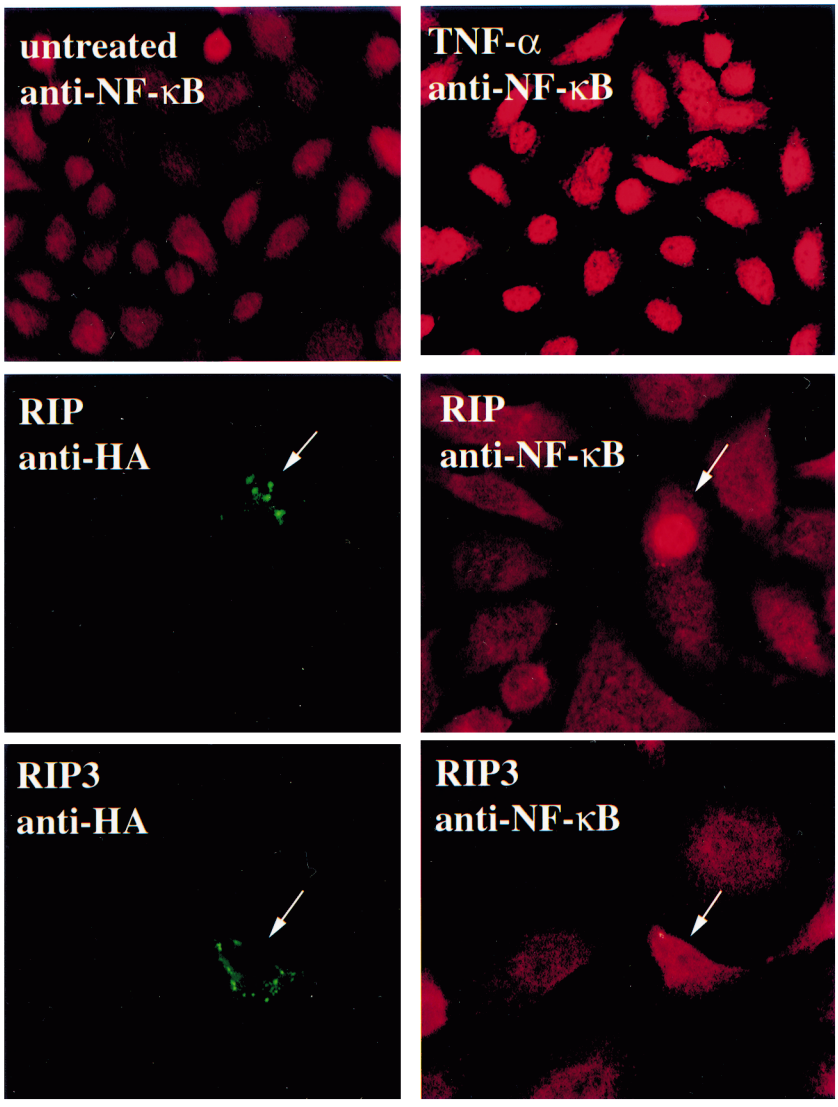

Fig. 4. RIP3 induction of NF-κB. HeLa cells (2×10^5) were transfected with 1 μg of pMH-*rip*3, pMH-*rip* or with a control empty pTracer-SV-40 vector. As a positive control, untransfected cells were treated with 1500 U/ml of TNF-α for 5 h. Twenty-four hours post-transfection, the cells were immuno-stained with the mouse monoclonal HA antibody as well as a rabbit polyclonal antibody against NF-κB. Staining was visualized using FITC- and Cy-3-conjugated antibodies against mouse and rabbit, respectively. Representative micrographs (60× objective) are shown for the indicated treatments. Green FITC staining is the HA staining while red Cy-3 staining is the NF-κB staining. Arrow bars point to co-stained cells.

main, a point mutant was made with double amino acid substitutions of the conserved tryptophans 434 and 478 (W434/W478) and was found to have reduced apoptotic activity. This raises the possibility that the C-terminus of RIP3 can have a biochemical role analogous to other death domains.

To address the mechanism of RIP3-mediated apoptosis, the effects of known apoptotic inhibitors were examined. The anti-apoptotic Bcl-2 family members, Bcl-2 and Bcl-x_L, which inhibit apoptosis triggered by many stimuli, were capable of blocking RIP3-mediated apoptosis. This suggests that RIP3 functions upstream to Blc-2 family members in apoptotic signaling (Table 1). Co-expression of dominant-negative FADD (FADD-DN), which inhibits the apoptotic pathways initiated by TNF-α, Fas, and RIP [14,20,21], also suppressed apoptosis triggered by RIP3 (Table 1). The dependence of caspases on RIP3-mediated apoptosis was tested using both general and specific caspase inhibitors. The general caspase inhibitor Z-VAD was capable of suppressing RIP3-mediated apoptosis. More specific caspase inhibitors developed based upon distinct preferences in their cleavage site have been shown to be effective at selectively inhibiting caspase activation [22]. Some of these inhibitors were tested here for their ability to suppress RIP3-mediated apoptosis. The minimally effective amount of caspase inhibitor was used in order to maintain selectivity. Inhibition of RIP3 was observed by Z-DEVD, an inhibitor of caspase-3, -6, -7, -8, and -10, as well as by the caspase-2 inhibitor, Z-VDVAD (Table 1). In contrast, the caspase-6 inhibitor Z-VEID and caspase-8 inhibitor Z-IETD (Table 1) as well as the caspase-1 inhibitor Z-WEHD and the caspase-9 inhibitor Z-LEHD (data not shown) had little or no effect on RIP3-mediated apoptosis. Taken together, these data suggest that some or all of the set of caspases, caspase-2, -3, -7, and -10, are candidates for RIP3 signaling. These results appear to be consistent with the pathway involved in RIP-

mediated apoptosis which includes activation of caspase-2 through interaction with RAIDD [10,11]. However, both RIP [3,4] and its downstream effector, caspase-2 [23] are not required for TNF-α- or Fas-mediated apoptosis. This raises a question as to the physiological significance of the RIP family. One possibility is that they enhance the dominant FADD/caspase-8 pathway triggered by TNF-α. Thus, activation of caspase-2 via the RIP/RAIDD interaction provides additive signaling for apoptosis. However, it is also reasonable that the RIP family members play a more critical role in other death receptor-mediated cytotoxicity, such as DR5 and DR6, whose signaling pathways leading to cell death are largely unknown.

3.3. Sub-cellular localization of RIP3

To determine the sub-cellular localization of RIP3, the HA-tagged vector (pMH-*rip*3) was transfected into HeLa cells. Cells were maintained in the presence of the caspase inhibitors Z-VAD or Z-DEVD to protect them from apoptosis. Staining was performed by indirect immunofluorescence using a mouse monoclonal antibody against the HA epitope followed by a secondary FITC-conjugated goat anti-mouse antibody. HA-RIP3 was detected predominantly in a punctate pattern within the cytoplasm (Fig. 3) similar to that previously reported for RIP [2]. To investigate this in more detail, the staining was performed in conjunction with fluorescent markers for distinct sub-cellular organelles. No co-localization of RIP3 with the endoplasmic reticulum or Golgi apparatus was detected using the dyes Concanavalin A and wheat germ agglutinin (data not shown). However, RIP and RIP3 did co-localize with the mitochondrial selective dye, Mitotracker, which penetrates and stains functional mitochondria (Fig. 3). The similar localization of RIP and RIP3 is also consistent with their ability to interact [8,9] and suggests that the RIP–RIP3 interaction occurs at the mitochondrion.

The uptake of Mitotracker is dependent on the mitochondrion's activity which is often compromised during apoptosis. Caspase activation may occur both upstream or downstream of the loss of mitochondrial membrane potential [24]. Here, we observed in the presence of the general caspase inhibitor Z-VAD, RIP/RIP3 expressing cells had normal Mitotracker staining suggesting that RIP and RIP3 can activate caspases that are upstream of the mitochondrial events. To determine whether RIP and RIP3 were capable of disrupting mitochondrial activity, a more specific caspase inhibitor, Z-DEVD, was used. In the presence of Z-DEVD, RIP3 (Fig. 3) and RIP (data not shown) were still present in the punctate cytoplasmic regions. However, the Mitotracker staining in regions where RIP3 appeared to be more intense had disappeared. Thus the levels of RIP3 at the mitochondrion directly correlate with mitochondrial integrity suggesting a role for RIP3 in this part of the apoptotic process. Furthermore, the effects of RIP3 on the mitochondrion are vulnerable to Z-VAD, but not Z-DEVD-sensitive caspases. Interestingly, caspase-2 is one of the caspases normally found in the mitochondria and released upon apoptosis [25], which raises the possibility that RIP/RIP3 interaction with a RAIDD-like protein activates caspase-2 directly at the mitochondria rather than at the TNF receptor complex.

3.4. RIP3 induces NF-κB nuclear translocation

The ability of RIP3 to stimulate NF-κB activity has been somewhat controversial. Initial reports indicated that overexpression of RIP3 stimulated an NF-κB receptor construct [8]. Subsequently, it was found that RIP, but not RIP3 could induce NF-κB and that RIP3 could inhibit RIP-mediated NF-κB activation [9]. To help resolve this controversy, we examined the ability of RIP and RIP3 to translocate NF-κB from the cytoplasm to the nucleus. NF-κB is normally sequestered in the cytoplasm through an interaction with the inhibitory protein, I-κB. Phosphorylation of I-κB leads to its degradation by proteasomes resulting in the translocation of NF-κB to the nucleus. HeLa cells were transfected with vectors expressing either HA-RIP or HA-RIP3 and immuno-stained using both a mouse monoclonal HA antibody as well as a rabbit polyclonal antibody against NF-κB. As a positive control, we showed that treatment with TNF-α effectively induced NF-κB translocation (Fig. 4). Furthermore, overexpression of RIP induced NF-κB translocation in nearly all cells. RIP3, while not as potent as RIP, was still able to induce an increase in NF-κB nuclear translocation in about 50% of transfected cells. Untransfected cells, or cells transfected with an empty vector (pTracer-SV-40), showed relatively little NF-κB translocation (about 10%). These results clearly indicate that at a single cell level, overexpression of RIP3 is able to stimulate NF-κB and in summary highlight the dual functions of RIP3 in apoptosis and NF-κB activation.

Acknowledgements: We wish to thank W. Fieles and Dr. B. Speer for the RIP3 mutants and FADD-DN, as well as L. Hirata and P. Sherman for DNA sequencing.

References

[1] Nagata, S. (1997) Cell 88, 355–365.
[2] Stanger, B.Z., Leder, P., Lee, T.-H., Kim, E. and Seed, B. (1995) Cell 81, 513–523.
[3] Kelliher, M.A., Grimm, S., Ishida, Y., Kuo, F., Stanger, B.Z. and Leder, P. (1998) Immunity 8, 297–303.
[4] Ting, A.T., Pimentel-Muiños, F.X. and Seed, B. (1996) EMBO J. 15, 6189–6296.
[5] McCarthy, J.V., Ni, J. and Dixit, V.M. (1998) J. Biol. Chem. 273, 16968–16975.
[6] Inohara, N., del Paso, L., Koseki, T., Chen, S. and Nuñez, G. (1998) J. Biol. Chem. 273, 12296–12300.
[7] Thome, M., Hofmann, K., Burns, K., Martinon, F., Bodmer, J.L., Mattmann, C. and Tschopp, J. (1998) Curr. Biol. 8, 885–888.
[8] Yu, P.W., Huang, B.C.B., Shen, M., Quast, J., Chan, E. and Xu, X. et al. (1999) Curr. Biol. 9, 539–542.
[9] Sun, X., Lee, J., Navas, T., Baldwin, D.T., Stewart, T.A. and Dixit, V.M. (1999) J. Biol. Chem. 274, 16871–16875.
[10] Duan, H. and Dixit, V. (1997) Nature 385, 86–89.
[11] Ahmad, M., Srinivasula, S.M., Wang, L., Talanian, R.V., Litwack, G., Fernandes-Alnemri, T. and Alnemri, E.S. (1997) Cancer Res. 57, 615–619.
[12] Huang, B., Eberstadt, M., Olejniczak, E.T., Meadows, R.P. and Fesik, S.W. (1996) Nature 384, 638–641.
[13] Chou, J.J., Matsuo, H., Duan, H. and Wagner, G. (1998) Cell 94, 171–180.
[14] Hsu, H., Shu, H.-B., Pan, M.-G. and Goeddel, D.V. (1996) Cell 84, 299–308.
[15] Mutirangura, A., Pornthansakasem, W., Sriuranpong, V., Supiyaphun, P. and Voravud, N. (1998) Int. J. Cancer 78, 153–156.
[16] Matsuo, Y., Tomiyasu, T., Shirakawa, F., Yamashita, U., Sagawawa, K., Yokoyama, M.M. and Minowada, J. (1989) Hum. Cell 2, 423–429.
[17] Hecht, F., Morgan, R., Hecht, B.K. and Smith, S.D. (1984) Science 226, 1445–1447.
[18] Yunis, J.J. (1988) Cancer Detect. Prev. 12, 291–296.
[19] Watanabe-Fukunaga, R., Brannan, C.I., Copeland, N.G., Jenkins, N.A. and Nagata, S. (1992) Nature 356, 314–317.

[20] Chinnaiyan, A.M., Tepper, C.G., Seldin, M.F., O'Rourke, K., Kischkel, F.C., Hellbardt, S., Krammer, P.H., Peter, M.E. and Dixit, V.M. (1996) J. Biol. Chem. 271, 4961–4965.
[21] Grimm, S., Stanger, B.Z. and Leder, P. (1996) Proc. Natl. Acad. Sci. USA 93, 10923–10927.
[22] Thornberry, N.A., Rano, T.A., Peterson, E.P., Rasper, D.M., Timkey, T., Garcia-Calvo, M., Houtzager, V.M., Nordstrom, P.A., Roy, S., Vaillancourt, J.P., Chapman, K.T. and Nicholson, D.W. (1997) J. Biol. Chem. 272, 17907–17911.
[23] Bergeron, L., Perez, G.I., Macdonald, G., Shi, L., Sun, Y., Jurisicova, A. and Varmuza, S. et al. (1998) Genes Dev. 12, 1304–1314.
[24] Green, D.R. (1998) Cell 94, 695–698.
[25] Susin, S.A., Lorenzo, H.K., Zamzami, N., Marzo, I., Brenner, C. and Larochette, N. et al. (1999) J. Exp. Med. 2, 381–393.